

Recognition and One-Pot Extraction of Right- and Left-Handed Semiconducting Single-Walled Carbon Nanotube Enantiomers Using Fluorene-Binaphthol Chiral Copolymers

Kojiro Akazaki,[†] Fumiyuki Toshimitsu,[†] Hiroaki Ozawa,[†] Tsuyohiko Fujigaya,[†] and Naotoshi Nakashima^{*,†,‡,§}

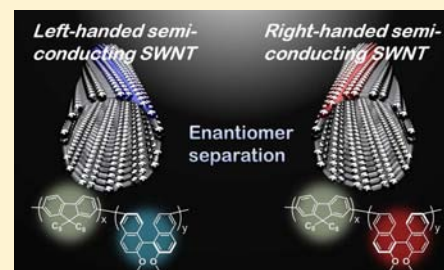
[†]Department of Applied Chemistry, Graduate School of Engineering, Kyushu University, Fukuoka 819-0395, Japan

[‡]International Institute for Carbon-Neutral Energy Research (WPI-I2CNER), Kyushu University, Fukuoka 819-0395, Japan

[§]Japan Science and Technology Agency (JST), Core Research of Evolutional Science & Technology (CREST), 5 Sanbancho, Chiyoda-ku, Tokyo 102-0075, Japan

Supporting Information

ABSTRACT: Synthesized single-walled carbon nanotubes (SWNTs) are mixtures of right- and left-handed helicity and their separation is an essential topic in nanocarbon science. In this paper, we describe the separation of right- and left-handed semiconducting SWNTs from as-produced SWNTs. Our strategy for this goal is simple: we designed copolymers composed of polyfluorene and chiral bulky moieties because polyfluorenes with long alkyl-chains are known to dissolve only semiconducting SWNTs and chiral binaphthol is a so-called BINAP family that possesses a powerful enantiomer sorting capability. In this study, we synthesized 12 copolymers, (9,9-dioctylfluorene-2,7-diyl) x ((*R*)- or (*S*)-2,2'-dimethoxy-1,1'-binaphthalen-6,6'-diyl) y , where x and y are copolymer composition ratios. It was found that, by a simple one-pot sonication method, the copolymers are able to extract either right- or left-handed semiconducting SWNT enantiomers with (6,5)- and (7,5)-enriched chirality. The separated materials were confirmed by circular dichroism, vis-near IR and photoluminescence spectroscopies. Interestingly, the copolymer showed inversion of SWNT enantiomer recognition at higher contents of the chiral binaphthol moiety. Molecular mechanics simulations reveal a cooperative effect between the degree of chirality and copolymer conformation to be responsible for these distinct characteristics of the extractions. This is the first example describing the rational design and synthesis of novel compounds for the recognition and simple sorting of right- and left-handed semiconducting SWNTs with a specific chirality.



INTRODUCTION

Single-walled carbon nanotubes (SWNTs) are one of the most promising materials in the field of nanoscience and nanotechnology due to their remarkable electronic, mechanical, thermal and optical properties.^{1–6} Their structural identities, such as diameter, chiral angle and fundamental properties are described by a chirality index (n,m).^{7,8} As-synthesized SWNTs are usually mixed racemic mixtures of semiconducting- and metallic-SWNTs with many chirality indices (n,m).^{9,10} These SWNT enantiomers exhibit corresponding circular dichroism (CD)^{11,12} as can be seen in many chiral compounds. Recently, several challenges describing the separation of the racemic mixtures of SWNTs into each enantiomer have been reported. Komatsu et al.^{12,13} used chiral diporphyrin molecules to separate the left- and right- racemic mixtures. Hersam et al.^{14,15} and Weisman et al.¹⁶ employed a density gradient ultracentrifugation (DGU) technique and an improved non-linear DGU gradient using mixed surfactants of sodium cholate and sodium dodecyl sulfate, respectively, for sorting the SWNT enantiomers. However, the DGU method is rather complex and requires long procedures. In addition, it needs a density gradient medium such as iodixanol, which is very expensive and

remains as an impurity even after separation. More importantly, in many cases, sorted right- and left-handed SWNT enantiomers contain both metallic and semiconducting SWNTs. However, to our knowledge, no report describing a simple one-pot separation of semiconducting- or metallic SWNT enantiomers from a mixture has been published.

Polyfluorene-based copolymers are intensively focused due to their highly specific sorting ability toward semiconducting SWNTs.^{17,18} We have previously demonstrated a rational method for the selective recognition and solubilization of specific chirality of (n,m)SWNTs with a series of systematically designed and synthesized fluorene-based copolymers.¹⁹

With this insight, our goal in this study is a simple one-pot separation of semiconducting left- or right-handed SWNT enantiomers with a specific (n,m) chirality. Our concept for the goal is based on the combination of hybridizing chirality sorting and enantioselective extraction; namely, we introduced a chiral binaphthol moiety, (*R*)- or (*S*)-2,2'-dimethoxy-1,1'-binaphthyl-6,6'-diyl (denoted RBN and SBN, respectively), to a fluorene

Received: May 2, 2012

Published: July 12, 2012

polymer (poly-9,9-dioctyl-2,7-fluorene, PFO). PFO and its derivatives^{20–26} are known to dissolve only semiconducting SWNTs and RBN and SBN are part of the BINAP family of compounds that possess powerful enantiomer recognizing ability.^{27–29} To realize our concept, as shown in Figure 1, we

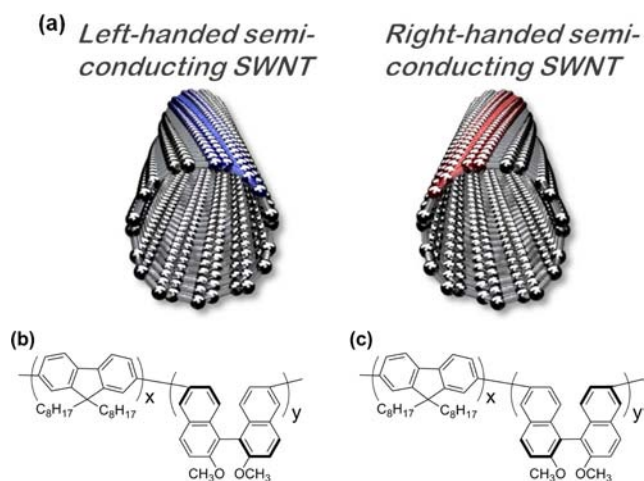


Figure 1. Schematic drawing of (a) semiconducting SWNT enantiomers and chemical structures of (b) (PFO)_x(RBN)_y and (c) (PFO)_x(SBN)_y.

synthesized twelve novel copolymers, (PFO)_x(RBN)_y and (PFO)_x(SBN)_y, in which x and y are the copolymer composition ratios. The copolymers successfully extracted only semiconducting SWNT enantiomers by simple sonication in toluene and no further purification was needed. In particular, we found that the proportion of chiral binaphthol moieties exhibited a dramatic influence on the recognition/extraction of the SWNT enantiomers. To explain the selectivity of our copolymers, we used Molecular Mechanics methods to model the conformation of each copolymer on the SWNTs in accordance with typical experimental conditions. The calculation demonstrated that the driving force of enantioselective sorting was governed by both chiral interactions and copolymer wrapping. These effects altered cooperatively upon changing composition ratio of the copolymers.

RESULTS AND DISCUSSION

Selective Recognition/Extraction of SWNTs by Chiral Copolymers. We synthesized twelve copolymers composed of PFO and chiral binaphthol moieties with different composition ratios using the Yamamoto coupling reaction. The resulting ratios of the PFO(x) and RBN(y) (or SBN(y)) were determined quantitatively by ¹H NMR spectroscopy: for (PFO)_x(RBN)_y, ($x:y$) = (86:14), (76:24), (71:29), (68:32), (61:39) and (44:56); for (PFO)_x(SBN)_y, ($x:y$) = (85:15), (72:28), (65:35), (55:45), (51:49) and (47:53). Throughout this paper, the copolymers are named based on the percentage of each comonomer unit. The details of the synthetic procedures and the analytical data are described in the Experimental Section and the Supporting Information. The UV–vis absorption and circular dichroism (CD) spectra of the typical synthesized copolymers dissolved in toluene are shown in Figure 2(a,b), in which (PFO)_x(RBN)_y and (PFO)_x(SBN)_y show almost mirror-imaged CD spectra (for absorption and CD spectra of six other copolymers, see Supporting Information, Figures S1 and S2). The introduction of the

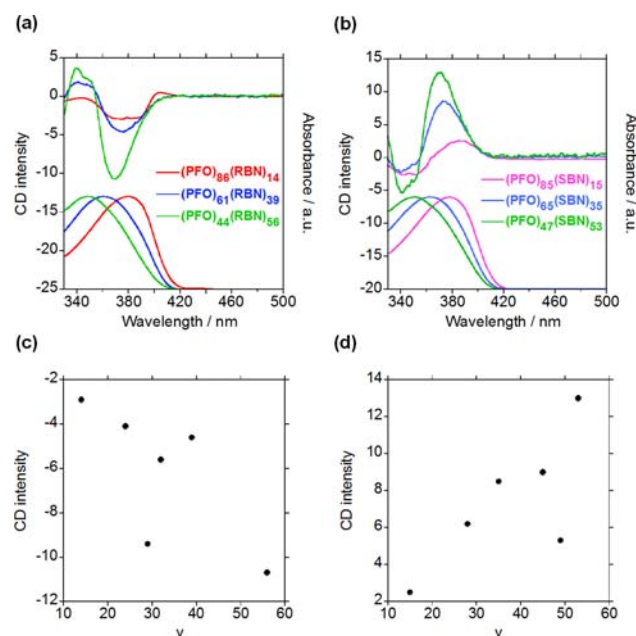


Figure 2. UV–vis absorption and CD spectra of (a) (PFO)_x(RBN)_y ($x:y$ = 86:14, 61:39 and 44:56) and (b) (PFO)_x(SBN)_y ($x:y$ = 85:15, 65:35 and 47:53). CD spectra are normalized based on the absorbance intensity of the copolymers at maximum wavelength. The CD intensity is plotted as a function of (c) RBN and (d) SBN ratios.

bulky binaphthol moiety caused a blue shift due to a decreased effective π -conjugation, which suggests that the copolymers are allowed to have more conformations than normal PFOs. The CD intensity also reflected the proportion of chiral RBN and SBN moieties as shown in Figure 2(c,d), in which the CD intensity was plotted as a function of RBN or SBN ratios.

The vis-NIR absorption spectra of the solubilized SWNTs are shown in Figure 3, in which we observe the first (E_{11}^s) and second (E_{22}^s) semiconducting bands and almost no metallic band in the range of 400–550 nm (for full range absorption spectra, see the Supporting Information, Figure S3). These results clearly indicate that the synthesized copolymers dissolved semiconducting SWNTs with a high selectivity, as with normal PFO compounds. Judging from the absorbance intensity of SWNTs solubilized by normal PFO and (PFO)₆₁(RBN)₃₉, the introduction of binaphthol moiety on the copolymer did not significantly affect SWNT dispersion ability (see Supporting Information, Figure S4). Furthermore, the introduction of the RBN or SBN to the PFO, depending on the composition ratios of the copolymers, gradually altered the preferred chirality indices (n,m) in the extracted SWNTs. To assign the precise chirality index and the relative amount of the solubilized SWNT species, photoluminescence (PL) spectroscopy was carried out on all the 12 samples. The typical two-dimensional PL mapping of the copolymer-solubilized SWNTs is shown in Figure 4 and the calibrated content of the SWNT species assessed from the PL mappings are summarized in Table 1. It is evident that the composition ratios of the comonomer units plays an important role in sorting the SWNT chirality, as seen in our previous report on fluorene-based copolymers.¹⁹ The present (PFO)_x(RBN/SBN)_y copolymers with the higher PFO contents were found to enrich (7,5)SWNTs, and the increase of RBN/SBN composition ratios enabled the extraction of (6,5), (7,6) and (8,6)SWNTs.

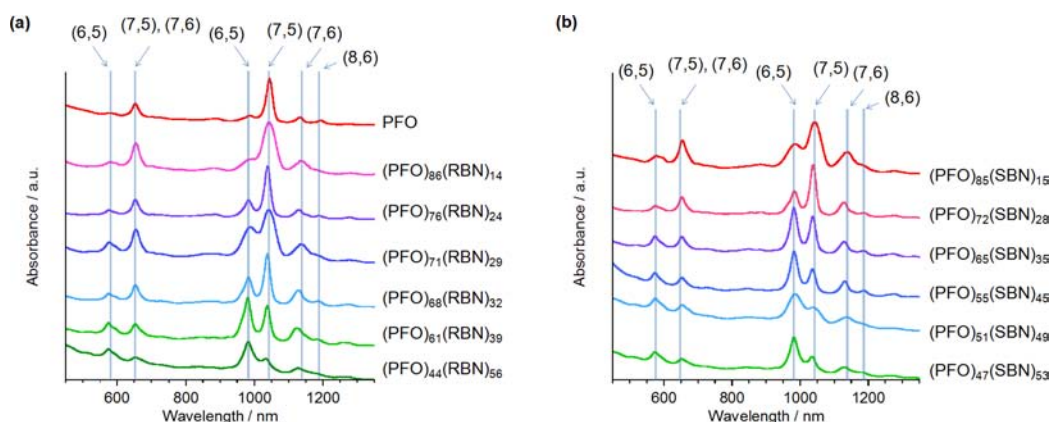


Figure 3. Absorption spectra of SWNTs solubilized by (a) PFO, $(\text{PFO})_x(\text{RBN})_y$ ($x:y = 86:14, 76:24, 71:29, 68:32, 61:39$ and $44:56$) and (b) $(\text{PFO})_x(\text{SBN})_y$ ($x:y = 85:15, 72:28, 65:35, 55:45, 51:49$ and $47:53$).

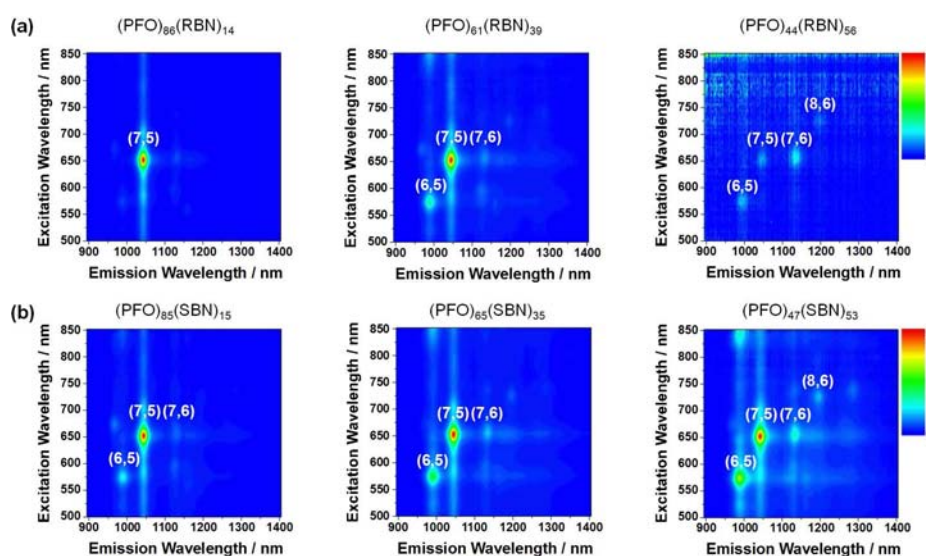


Figure 4. 2D-Photoluminescence (PL) mapping of SWNTs solubilized by copolymers (a) $(\text{PFO})_x(\text{RBN})_y$ ($x:y = 86:14, 61:39$ and $44:56$) and (b) $(\text{PFO})_x(\text{SBN})_y$ ($x:y = 85:15, 65:35$ and $47:53$).

Table 1. Calibrated Content of the SWNT Species Deduced from the PL Mappings of the Samples Prepared Using Copolymers $(\text{PFO})_x(\text{RBN})_y$ or $(\text{PFO})_x(\text{SBN})_y$ in Toluene

chiral index (n,m)	calibrated content / %			chiral index (n,m)	calibrated content / %		
	$(\text{PFO})_{86}(\text{RBN})_{14}$	$(\text{PFO})_{61}(\text{RBN})_{39}$	$(\text{PFO})_{44}(\text{RBN})_{56}$		$(\text{PFO})_{85}(\text{SBN})_{15}$	$(\text{PFO})_{65}(\text{SBN})_{35}$	$(\text{PFO})_{47}(\text{SBN})_{53}$
(6,5)	4.27	27.2	18.3	(6,5)	38.0	25.9	23.1
(7,5)	82.7	39.6	18.7	(7,5)	48.7	50.7	44.5
(7,6)	10.6	23.4	39.0	(7,6)	9.88	16.4	19.4
(8,6)	2.46	9.76	24.0	(8,6)	3.39	6.98	13.1

Figure 5 shows the vis-NIR absorption and CD spectra (intensity is normalized at 574 nm) of the SWNTs solubilized by $(\text{PFO})_{61}(\text{RBN})_{39}$ and $(\text{PFO})_{65}(\text{SBN})_{35}$, in which evident CD peaks are observed in the region of the second (E_{22}^s) and first (E_{11}^s) semiconducting bands of the SWNTs (for absorption and CD spectra of the SWNTs solubilized with ten other copolymers, see Supporting Information, Figures S5 and S6).

To eliminate the contribution of induced CD³⁰ from the chiral copolymers on the SWNT/copolymer composites, an in situ copolymer exchange reaction by using the incorporation of an optically neutral achiral copolymer was conducted. Since in our study, the chiral copolymers that wrapped SWNTs were

unable to be removed by washing technique³¹ because of the strong binding between the copolymers and the SWNTs. Here, poly(9,9-dioctylfluorene-2,7-diyl-2,2'-bipyridine-6,6'-diyl) (**PFO-Bpy**) (for chemical structure and simulated stabilizing energy on the SWNTs, see Supporting Information, Figure S7 and Table S1) was used as an achiral copolymer to replace the chiral copolymers on the solubilized (6,5)SWNTs because it has a stronger affinity to the (6,5)SWNTs and causes an indicative absorption peak shift (~ 9 nm) relative to the pristine (6,5)SWNTs in the NIR region.²³ As a control, we found no optical activity over the same spectral range in **PFO-Bpy**-solubilized SWNTs, that is, **PFO-Bpy** extracted racemic (6,5)SWNTs. The obtained vis-NIR absorption spectra of the

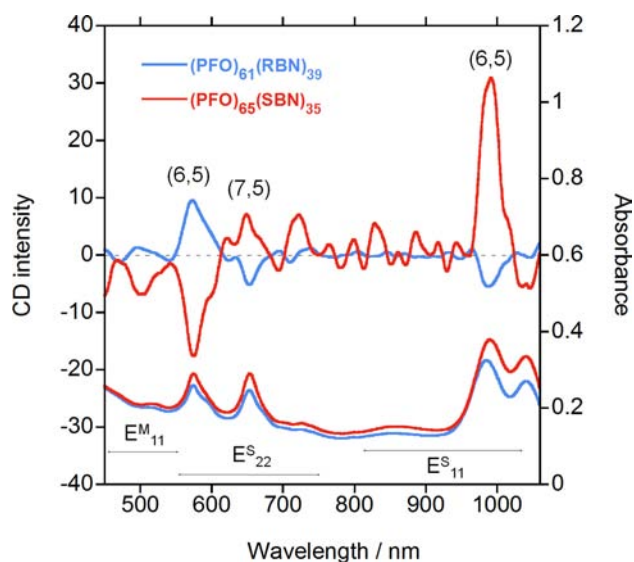


Figure 5. Absorption and CD spectra of SWNTs extracted with $(\text{PFO})_{61}(\text{RBN})_{39}$ and $(\text{PFO})_{65}(\text{SBN})_{35}$. CD spectra are normalized based on the absorbance intensity of the SWNTs at 574 nm.

E_{11}^s region of the (6,5)SWNT after the copolymer exchange that was caused by adding excess amounts of PFO-Bpy into the SWNTs/ $(\text{PFO})_{61}(\text{RBN})_{39}$ solution was almost identical to the original chiral copolymer to the PFO-Bpy (for absorption and CD spectra of the SWNTs extracted by $(\text{PFO})_{61}(\text{RBN})_{39}$ before and after the addition of PFO-Bpy, see Supporting Information, Figures S8). Furthermore, the CD spectral change was not significant after the addition of the PFO-Bpy to the solution; specifically, the CD intensities around 574 nm were 9.52 and 9.35 before and after the addition of the PFO-Bpy respectively. Consequently, it is evident that the observed spectra are not a result of induced CD but originate from the E_{22}^s band of the enantiomers of the semiconducting (6,5)SWNTs (around 574 nm) and (7,5)SWNTs (around 653 nm).

We now discuss the effect of the composition ratios of $(\text{PFO})_x(\text{RBN})_y$ and $(\text{PFO})_x(\text{SBN})_y$ on the CD intensity of the extracted SWNT enantiomers. This result is shown in Figure 6 as a plot of CD intensity at 574 nm of the extracted SWNTs versus composition ratios (y) of RBN or SBN in the copolymers. In this paper, SWNT enantiomers are labeled as (+) or (−) according to whether their CD signals at the E_{22}^s band are positive or negative. It was to our surprise that the CD intensity of the solubilized SWNT enantiomers was not simply proportional to the composition ratios of the chiral binaphthol in the copolymers. For $(\text{PFO})_x(\text{RBN})_y$, with the increase in the composition ratios of the RBN moiety (y) of up to 39%, the (+)SWNTs were enriched, whereas the CD signal dramatically inverted at higher y values ending up at (−)SWNTs enrichment with the copolymer $(\text{PFO})_{44}(\text{RBN})_{56}$. Similar behavior was also observed when $(\text{PFO})_x(\text{SBN})_y$ was used; namely, as the y values in the $(\text{PFO})_x(\text{SBN})_y$ changed from 15 to 35, the amount of (−)SWNTs were multiplied, whereas copolymers with higher y values extracted (+)SWNTs. Considering the large structural change of the copolymers upon altering the composition ratios, as indicated by the blue shift in Figure 2(a,b), it is suggested that the ratios of the chiral moiety and the conformation of the copolymers cooperatively determine the affinity to the handedness of the SWNT enantiomers. The drastic but still controllable preference of

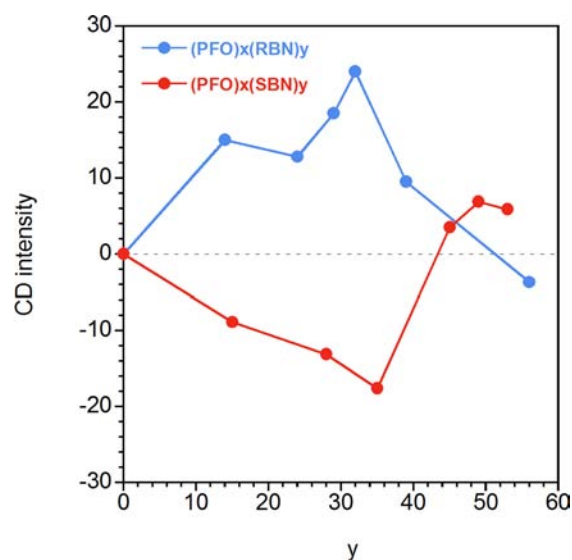


Figure 6. CD intensity at around 574 nm of the extracted SWNTs as a function of composition ratios of RBN or SBN in the copolymer.

the chiral copolymers for extracting SWNT enantiomers allows desired separation parameters to be identified and optimized. To estimate the performance of enantioselective extraction of the SWNTs by our chiral copolymers, we applied the following eq 1, which was presented by Wang et al.,¹³ placing optical purity of the extracted enantiomer as CD_{norm}

$$CD_{\text{norm}} = (CD_{\text{raw}}/L_{\text{CD}})/(A_{E_{22}}/L_{\text{abs}}) \quad (1)$$

where CD_{raw} is the CD intensity at 574 nm of the E_{22}^s transition, $A_{E_{22}}$ is the background-corrected absorption intensity at 574 nm of the E_{22}^s transition and L_{CD} and L_{abs} are the path lengths of the optical cell used in the measurements of CD and absorbance. Our results and previously reported values using given methods are summarized in Table 2. In this study, a maximum enantiomer purity (CD_{norm}) of 24 mdeg was obtained by using $(\text{PFO})_{68}(\text{RBN})_{32}$ on (+)(6,5)SWNT, which is comparable to those reported by Komatsu et al. using chiral diporphyrins¹³ but lower than those obtained by Hersam et al.^{14,15} and Weisman et al.¹⁶ using the DGU method. Our method, however, is simple and the extracted nanotubes are solely semiconducting enantiomeric SWNTs, which are both great advantages of this study.

Molecular Mechanics Simulations. Our copolymers exhibited two intriguing SWNT recognition/extraction behaviors: one is specific enantiomer recognition and the other is drastic inversion of preference between the (R)- or (S)-copolymers for the (+)- or (−)SWNTs, depending on the copolymer composition ratios. In order to understand the origin of the enantiomer recognition behavior of the copolymers synthesized in this study, molecular mechanics simulations using the OPLS2005 force field³² were utilized to model the interactions between the (6,5)SWNT enantiomers and the copolymers. PFO was employed as a comparison. The initial structures of the polymers were determined by the composition ratio and the average molecular weight of the synthesized polymers and the length was set at around 86 nm. The length of (6,5)SWNTs used in this calculation was 172 nm so as to keep copolymers around the center of the SWNT surface and enantiomers were identical except for helicity. The

Table 2. Comparison of Enantiomer Purity of (6,5)SWNTs Extracted by Four Different Methods

method	CD _{raw} /mdeg	L _{CD} /cm	A _{E₂₂}	L _{abs} /cm	CD _{norm} /mdeg	reference
DGU	-41.6	1.0	0.77	1.0	54	ref 15
DGU	20	1.0	0.55	1.0	36	ref 16
Molecular recognition	4.0	10	0.017	1.0	24	ref 13
Enantiomer separation using (PFO) ₆₈ (RBN) ₃₂	0.60	1.0	0.025	1.0	24	This study

Table 3. Calculated Potential and Binding Energies Between (6,5)SWNT Enantiomers with (PFO)₆₀(RBN)₄₀

(6,5) SWNTs	potential energy of SWNT (E _{SWNT})/kcal mol ⁻¹	potential energy of (PFO) ₆₀ (RBN) ₄₀ (E _{polymer})/kcal mol ⁻¹	total potential energy (E _{polymer} + E _{SWNT})/kcal mol ⁻¹	potential energy of complex (E _{complex})/kcal mol ⁻¹	binding energy E _{bind} = E _{complex} - (E _{polymer} + E _{SWNT})/kcal mol ⁻¹
Left-handed	88163	1437	89600	88967	-633
Right-handed	88163	1437	89600	88979	-621

Table 4. Calculated Potential and Binding Energies between (6,5)SWNT Enantiomers with (PFO)₆₀(SBN)₄₀

(6,5) SWNTs	potential energy of SWNT (E _{SWNT})/kcal mol ⁻¹	potential energy of (PFO) ₆₀ (SBN) ₄₀ (E _{polymer})/kcal mol ⁻¹	total potential energy (E _{polymer} + E _{SWNT})/kcal mol ⁻¹	potential energy of complex (E _{complex})/kcal mol ⁻¹	binding energy E _{bind} = E _{complex} - (E _{polymer} + E _{SWNT})/kcal mol ⁻¹
Left-handed	88163	1437	89600	88981	-619
Right-handed	88163	1437	89600	88965	-635

Table 5. Calculated Potential and Binding Energies between (6,5)SWNT Enantiomers with the (PFO)₄₄(RBN)₅₆

(6,5) SWNTs	potential energy of SWNT (E _{SWNT})/kcal mol ⁻¹	potential energy of (PFO) ₄₄ (RBN) ₅₆ (E _{polymer})/kcal mol ⁻¹	total potential energy (E _{polymer} + E _{SWNT})/kcal mol ⁻¹	potential energy of complex (E _{complex})/kcal mol ⁻¹	binding energy E _{bind} = E _{complex} - (E _{polymer} + E _{SWNT})/kcal mol ⁻¹
Left-handed	88163	1566	89729	89102	-627
Right-handed	88163	1566	89729	89094	-635

Table 6. Calculated Potential and Binding Energies Between (6,5)SWNT Enantiomers with (PFO)₄₄(SBN)₅₆

(6,5) SWNTs	potential energy of SWNT (E _{SWNT})/kcal mol ⁻¹	potential energy of (PFO) ₄₄ (SBN) ₅₆ (E _{polymer})/kcal mol ⁻¹	total potential energy (E _{polymer} + E _{SWNT})/kcal mol ⁻¹	potential energy of complex (E _{complex})/kcal mol ⁻¹	binding energy E _{bind} = E _{complex} - (E _{polymer} + E _{SWNT})/kcal mol ⁻¹
Left-handed	88163	1566	89729	89081	-648
Right-handed	88163	1566	89729	89095	-634

binding energy (E_{bind}) of the wrapped SWNT was calculated by using eq 2

$$E_{\text{bind}} = E_{\text{complex}} - (E_{\text{SWNT}} + E_{\text{polymer}}) \quad (2)$$

where E_{complex}, E_{polymer} and E_{SWNT} represent the potential energies of the complex, polymer and SWNTs, respectively. Assuming that the same energy is obtained from identical conformation and neglecting periodic heterogeneous fluctuation on the surfaces of calculated SWNTs induced by their edge structures, the resulting binding energy could be considered as an indicator of chiral interactions between the copolymers and the SWNTs. As the representative copolymer of a lower content of RBN/SBN, (PFO)₆₀(RBN)₄₀ and (PFO)₆₀(SBN)₄₀ were modeled to simulate copolymers which extracted the SWNT enantiomers most efficiently in this study. The calculated potential energies using (PFO)₆₀(RBN)₄₀ are summarized in Table 3, in which greater binding energies (-633 kcal mol⁻¹) were obtained with the left-handed (6,5)SWNTs compared to that with the right-handed form (-621 kcal mol⁻¹). Contrasting behavior was observed when

(PFO)₆₀(SBN)₄₀ was modeled and the calculated binding energy with right-handed SWNTs was greater (-635 kcal mol⁻¹) than that with the left-handed SWNTs (-619 kcal mol⁻¹) (Table 4). For comparison, PFO was modeled in the calculation with each SWNT enantiomer. The E_{bind} values of the left-handed SWNTs and the right-handed SWNTs with PFO were -623 kcal mol⁻¹ and -625 kcal mol⁻¹, respectively. The obtained difference (~2 kcal mol⁻¹) is much smaller compared to that obtained with the chiral copolymers. Considering that the same energies were obtained for each enantiomer of the SWNTs and also (PFO)₆₀(RBN)₄₀ and (PFO)₆₀(SBN)₄₀ showed a negligible difference among their E_{polymer} values, all obtained results demonstrate the distinct enantiomer recognition ability of (PFO)₆₀(RBN)₄₀ and (PFO)₆₀(SBN)₄₀ on the (6,5)SWNT enantiomers. The dependency of stabilizing energy upon altering the sequence in the copolymer was also verified. Due to the fact that the binaphthol homopolymer was unable to synthesize in our synthetic condition, molecular mechanics simulations on two different sequences of (PFO)₆₀(RBN)₄₀, (denoted

(PFO)₆₀(RBN)₄₀₋₂ and (PFO)₆₀(RBN)₄₀₋₃, respectively) were carried out. It was revealed that these two copolymers gave almost similar tendency to that of (PFO)₆₀(RBN)₄₀; namely, greater binding energies ($-590 \text{ kcal mol}^{-1}$ for (PFO)₆₀(RBN)₄₀₋₂ and $-624 \text{ kcal mol}^{-1}$ for (PFO)₆₀(RBN)₄₀₋₃) were obtained for the left-handed (6,5)SWNTs compared to that of the right-handed isomer ($-582 \text{ kcal mol}^{-1}$ for (PFO)₆₀(RBN)₄₀₋₂ and $-621 \text{ kcal mol}^{-1}$ for (PFO)₆₀(RBN)₄₀₋₃) (see Supporting Information, Table S2, Table S3 and Figure S9). These results strongly suggest that our synthesized chiral copolymers possess SWNT enantiomer recognition ability. Further calculations were carried out for the (6,5)SWNT enantiomers with (PFO)₄₄(RBN)₅₆ and (PFO)₄₄(SBN)₅₆ to explain the enantiomer recognition inversion with changing copolymer ratios. The E_{bind} of the complex of (PFO)₄₄(RBN)₅₆ with right-handed SWNTs was $-635 \text{ kcal mol}^{-1}$ and with left-handed SWNTs resulted in lower value of $-627 \text{ kcal mol}^{-1}$. As expected, opposite behavior was observed when (PFO)₄₄(SBN)₅₆ was applied; the E_{bind} were -648 and $-634 \text{ kcal mol}^{-1}$ for the complex with left-handed SWNT and right-handed SWNT, respectively (Tables 5 and 6). This behavior agrees well with the experimental results and is illustrated by comparing the wrapping conformations, as shown in Figures 7 and 8. It is remarkable

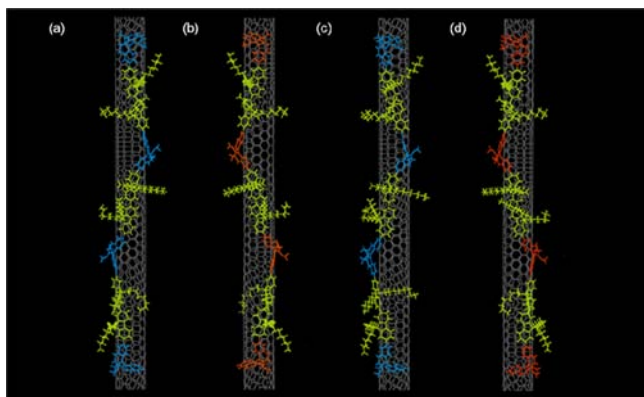


Figure 7. Modeled structures of (a) left-handed SWNT with (PFO)₆₀(RBN)₄₀, (b) left-handed SWNT with (PFO)₆₀(SBN)₄₀, (c) right-handed SWNT with (PFO)₆₀(RBN)₄₀, and (d) right-handed SWNT with (PFO)₆₀(SBN)₄₀.

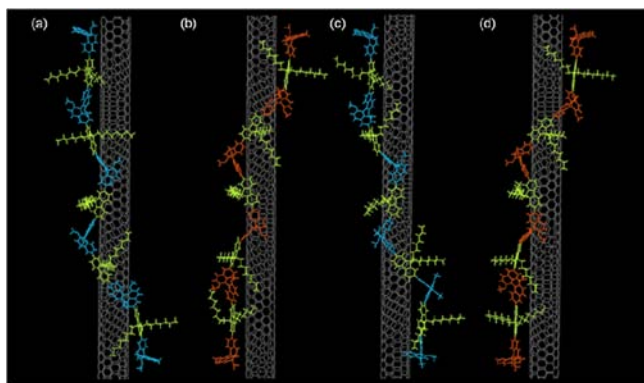


Figure 8. Modeled structures of (a) left-handed SWNT with the (PFO)₄₄(RBN)₅₆, (b) left-handed SWNT with (PFO)₄₄(SBN)₅₆, (c) right-handed SWNT with (PFO)₄₄(RBN)₅₆, and (d) right-handed SWNT with (PFO)₄₄(SBN)₅₆.

that the wrapping direction of the copolymers flipped by altering the composition ratios even though they have same chiral moieties; in other words, in the complex with (+)(6,5)SWNTs, (PFO)₆₀(RBN)₄₀ showed clockwise winding, while (PFO)₄₄(RBN)₅₆ wrapped the SWNT in the anticlockwise direction and other chiral copolymers synthesized in this study showed similar behavior. Such a dramatic conformation change switches the preferential interaction between the chiral copolymers and the SWNTs cooperatively with the degree of composition ratios of the chiral moiety in the copolymers. The relationship between the SWNT's handedness and optical activity is still remains to be elucidated conclusively, nevertheless we believe this approach and result might be a help to understand and direct interactions between tailored (co)-polymers and semiconducting/metallic (\pm)SWNTs with a specific chirality.

CONCLUSIONS

We have described a rational concept for the design of compounds that enable a simple one-pot separation of semiconducting (+)SWNTs and (–)SWNTs with a specific chirality. The designed and synthesized molecules were copolymers composed of PFO and chiral binaphthol moieties with different composition ratios. The key factors for the SWNT enantiomer separation and sorting of semiconducting SWNTs were the introduction of the bulky (*R*)- or (*S*)-chiral binaphthol- and PFO moieties. We discovered that by using the twelve selected copolymers with various composition ratios of PFO and binaphthol moieties, the (*R*)- or (*S*)-chiral copolymers extract either right- or left-handed SWNT enantiomers. This recognition inversion behavior was explained by a cooperative effect of chiral and conformational interactions, as revealed by molecular mechanics simulations based on binding energies. The essential concepts of this study will accelerate molecular solutions for enantioselective SWNT sorting of selected chiralities.

EXPERIMENTAL SECTION

Synthesis of Copolymers. (*R*)- and (*S*)-6,6'-Dibromo-2,2'-dimethoxy-1,1'-binaphthalene were synthesized according to the literature.³³ Chiral copolymers, (PFO)_{*x*}(RBN)_{*y*} and (PFO)_{*x*}(SBN)_{*y*} were synthesized via a Yamamoto coupling reaction.^{34,35} The synthesis procedure of (PFO)₆₁(RBN)₃₉ is described as follows: Ni(COD)₂ (100 mg, 0.36 mmol), 2,2'-dipyridyl (62 mg, 0.40 mmol), 1,5-cyclooctadiene (0.1 mL), dried DMF (1.5 mL) and dried toluene (3.0 mL) were placed in a flask and heated at 80 °C for 30 min under flowing nitrogen to obtain a dark purple complex, to which a mixed solution of 2,7-dibromo-9,9'-dioctylfluorene (55 mg) and (*R*)-6,6'-dibromo-2,2'-dimethoxy-1,1'-binaphthalene (39 mg) in dried DMF (0.5 mL) and dried toluene (0.5 mL) were added and then reacted at 80 °C for 24 h. After the reaction, the solution was poured into a mixed solution (150 mL) of 2 M HCl (50 mL), acetone (50 mL) and methanol (50 mL) to produce a precipitate, which was collected by filtration and then rinsed with acetone. The obtained solid was dissolved in chloroform and then reprecipitated from methanol to produce a yellowish solid (52 mg) as the final product. ¹H NMR (CDCl₃, 300 MHz): δ 8.30–7.40 (m, 3.2H), 3.80 (m, 1H), 2.04 (m, 1H), 1.35–0.936 (m, 5.2H), 0.916–0.437 (m, 2.6H). Yield: 52%. $M_n = 5377$, $M_w = 20658$, PDI = 3.84. The other 11 copolymers, (PFO)_{*x*}(RBN)_{*y*} and (PFO)_{*x*}(SBN)_{*y*}, were synthesized by a similar way. The composition ratios (*x*,*y*) of the copolymers were determined by their ¹H NMR spectra. (PFO)₈₆(RBN)₁₄: ¹H NMR (CDCl₃, 300 MHz): δ 8.3–7.40 (m, 10.2H), 3.80 (m, 1H), 2.04 (m, 4H), 1.35–0.936 (m, 35.7H), 0.916–0.437 (m, 38.9H). Yield: 52%, $M_n = 28514$, $M_w = 55618$, PDI = 1.95. (PFO)₇₆(RBN)₂₄: ¹H NMR (CDCl₃, 300 MHz):

δ 8.30–7.40 (m, 5.66H), 3.80 (m, 1H), 2.04 (m, 2.07H), 1.35–0.936 (m, 14.1H), 0.916–0.437 (m, 6.11H). Yield: 86%, $M_n = 23962$, $M_w = 85831$, PDI = 3.58. (PFO)₇₁(RBN)₂₉: ¹H NMR (CDCl₃, 300 MHz): δ 8.30–7.40 (m, 5.36H), 3.80 (m, 1H), 2.04 (m, 1.62H), 1.35–0.936 (m, 8.88H), 0.916–0.437 (m, 4.3H). Yield: 63%, $M_n = 16328$, $M_w = 42775$, PDI = 2.62. (PFO)₆₈(RBN)₃₂: ¹H NMR (CDCl₃, 300 MHz): δ 8.30–7.40 (m, 3.94H), 3.80 (m, 1H), 2.04 (m, 1.44H), 1.35–0.936 (m, 7.89H), 0.916–0.437 (m, 3.73H). Yield: 46%, $M_n = 9029$, $M_w = 30383$, PDI = 3.37. (PFO)₄₄(RBN)₅₆: ¹H NMR (CDCl₃, 300 MHz): δ 8.30–7.40 (m, 2.19H), 3.80 (m, 1H), 2.04 (m, 0.533H), 1.35–0.936 (m, 2.85H), 0.916–0.437 (m, 1.55H). Yield: 37%, $M_n = 2055$, $M_w = 11565$, PDI = 5.63. (PFO)₈₅(SBN)₁₅: ¹H NMR (CDCl₃, 300 MHz): δ 8.30–7.40 (m, 7.61H), 3.80 (m, 1H), 2.04 (m, 3.7H), 1.35–0.936 (m, 21.5H), 0.916–0.437 (m, 9.63H). Yield: 82%, $M_n = 20923$, $M_w = 51138$, PDI = 2.44. (PFO)₇₂(SBN)₂₈: ¹H NMR (CDCl₃, 300 MHz): δ 8.30–7.40 (m, 4.4H), 3.80 (m, 1H), 2.04 (m, 1.73H), 1.35–0.936 (m, 9.48H), 0.916–0.437 (m, 4.46H). Yield: 49%, $M_n = 12461$, $M_w = 36663$, PDI = 2.94. (PFO)₆₅(SBN)₃₅: ¹H NMR (CDCl₃, 300 MHz): δ 8.30–7.40 (m, 3.76H), 3.80 (m, 1H), 2.04 (m, 1.25H), 1.35–0.936 (m, 6.73H), 0.916–0.437 (m, 3.33H). Yield: 56%, $M_n = 9966$, $M_w = 24790$, PDI = 2.49. (PFO)₅₅(SBN)₄₅: ¹H NMR (CDCl₃, 300 MHz): δ 8.30–7.40 (m, 2.90H), 3.80 (m, 1H), 2.04 (m, 0.804H), 1.35–0.936 (m, 5.67H), 0.916–0.437 (m, 3.22H). Yield: 53%, $M_n = 4489$, $M_w = 14086$, PDI = 3.14. (PFO)₅₁(SBN)₄₉: ¹H NMR (CDCl₃, 300 MHz): δ 8.30–7.40 (m, 2.63H), 3.80 (m, 1H), 2.04 (m, 0.692H), 1.35–0.936 (m, 3.69H), 0.916–0.437 (m, 1.78H). Yield: 45%, $M_n = 3818$, $M_w = 24110$, PDI = 6.31. (PFO)₄₇(SBN)₅₃: ¹H NMR (CDCl₃, 300 MHz): δ 8.30–7.40 (m, 2.33H), 3.80 (m, 1H), 2.04 (m, 0.584H), 1.35–0.936 (m, 3.14H), 0.916–0.437 (m, 1.55H). Yield: 47%, $M_n = 3292$, $M_w = 16873$, PDI = 5.13.

Enantioselective Separation of (n,m)SWNTs. CoMoCAT-SWNTs (SWEENTSG65, SouthWest NanoTechnologies, Co.) were purchased from Aldrich and used as received. A typical procedure for the SWNT dissolution using the copolymers is as follows: the SWNTs (1 mg) and the copolymer (3 mg) were sonicated in toluene (3 mL) for 1 h and the dispersion was centrifuged at 10000× g for 1 h followed by collection of the supernatant (upper 80%) for measurements. Vis-NIR absorption, circular dichroism and PL spectra were measured using a spectrophotometer (JASCO, type V-570), a circular dichroism spectropolarimeter (JASCO, type J-820) and a spectrofluorometer equipped with a liquid-nitrogen-cooled InGaAs near-IR detector (Horiba-Jobin Yvon, SPEX Fluorolog-3-NIR), respectively. The excitation and emission wavelengths for PL measurements were in the range of 500–850 and 900–1400 nm, respectively.

Molecular Mechanics Simulations. The molecular mechanics simulations were carried out using MacroModel (Infocom, version 8.6) with the OPLS-2005 force field. Dielectric constants were kept at 2.3. Minimization on the calculation was carried out using the Polak-Ribiere conjugate gradient with a convergence threshold on the gradient of 0.05 kJ mol⁻¹. Default values were used for all other parameters.

■ ASSOCIATED CONTENT

Supporting Information

UV-vis-NIR absorption and CD spectra of all the 12 copolymers, UV-vis-NIR absorption, CD spectra of in situ copolymer exchange experiment, additional modeled structures of left- and right handed SWNTs with the copolymers, and calculated potential and binding energies of SWNTs with PFO-Bpy and with the additional copolymers. This material is available free of charge via the Internet at <http://pubs.acs.org>.

■ AUTHOR INFORMATION

Corresponding Author

nakashima-tcm@mail.cstm.kyushu-u.ac.jp

Notes

The authors declare no competing financial interest.

■ ACKNOWLEDGMENTS

This work was supported by a Grant-in-Aid for Scientific Research (B) (No. 17205014 for N.N.) and the Nanotechnology Network Project (Kyushu-area Nanotechnology Network) from the Ministry of Education, Culture, Sports, Science and Technology, Japan. We acknowledge Professor A. Robertson for his helpful comments, and Professors M. Goto and N. Kimizuka of Kyushu University for use of CD spectropolarimeter.

■ REFERENCES

- (1) Dai, H. *Acc. Chem. Res.* **2002**, *35*, 1035–1044.
- (2) Gao, X.; Li, K. *Int. J. Solids Struct.* **2003**, *40*, 7329–7337.
- (3) Zhao, X.; Lu, X.; Tze, W. T. Y.; Wang, P. *Biosens. Bioelectron.* **2010**, *25*, 2343–2350.
- (4) Fujigaya, T.; Okamoto, M.; Nakashima, N. *Carbon* **2009**, *47*, 3227–3232.
- (5) Okamoto, M.; Fujigaya, T.; Nakashima, N. *Small* **2009**, *5*, 735–740.
- (6) Hong, H.; Gao, T.; Cai, W. *Nano Today* **2009**, *4*, 252–261.
- (7) Odom, T. W.; Huang, J.-lin; Kim, P.; Lieber, C. M. *Nature* **1998**, *391*, 62–64.
- (8) Ouyang, M. I. N.; Huang, J.-lin; Lieber, C. M. *Acc. Chem. Res.* **2002**, *35*, 1018–1025.
- (9) Tasaki, S.; Maekawa, K.; Yamabe, T. *Phys. Rev. B* **1998**, *57*, 9301–9318.
- (10) Samsonidze, G.; Grüneis, A.; Saito, R.; Jorio, A.; Souza Filho, A.; Dresselhaus, G.; Dresselhaus, M. *Phys. Rev. B* **2004**, *69*, 205402–1–205402–11.
- (11) Sánchez-Castillo, A.; Román-Velazquez, C. E.; Noguez, C. *Phys. Rev. B* **2006**, *73*, 045401–1–045401–7.
- (12) Peng, X.; Komatsu, N.; Bhattacharya, S.; Shimawaki, T.; Aonuma, S.; Kimura, T.; Osuka, A. *Nat. Nanotechnol.* **2007**, *2*, 361–5.
- (13) Wang, F.; Matsuda, K.; Rahman, A. F. M. M.; Peng, X.; Kimura, T.; Komatsu, N. *J. Am. Chem. Soc.* **2010**, *132*, 10876–10881.
- (14) Green, A. A.; Hersam, M. C. *Adv. Mater.* **2011**, *23*, 2185–2190.
- (15) Green, A.; Duch, M. C.; Hersam, M. C. *Nano Res.* **2009**, *2*, 69–77.
- (16) Ghosh, S.; Bachilo, S. M.; Weisman, R. B. *Nat. Nanotechnol.* **2010**, *5*, 443–450.
- (17) Nish, A.; Hwang, J.; Doig, J.; Nicholas, R. J. *Nat. Nanotechnol.* **2007**, *2*, 640–646.
- (18) Chen, F.; Wang, B.; Chen, Y.; Li, L.-J. *Nano Lett.* **2007**, *7*, 3013–3017.
- (19) Ozawa, H.; Fujigaya, T.; Niidome, Y.; Hotta, N.; Fujiki, M.; Nakashima, N. *J. Am. Chem. Soc.* **2011**, *133*, 2651–2657.
- (20) Hwang, J.-Y.; Nish, A.; Doig, J.; Douven, S.; Chen, C.-W.; Chen, L.-C.; Nicholas, R. J. *J. Am. Chem. Soc.* **2008**, *130*, 3543–3553.
- (21) Stürzl, N.; Hennrich, F.; Lebedkin, S.; Kappes, M. M. *J. Phys. Chem. C* **2009**, *113*, 14628–14632.
- (22) Berton, N.; Lemasson, F.; Tittmann, J.; St, N.; Hennrich, F.; Kappes, M. M.; Mayor, M. *Chem. Mater.* **2011**, *23*, 2237–2249.
- (23) Ozawa, H.; Ide, N.; Fujigaya, T.; Niidome, Y.; Nakashima, N. *Chem. Lett.* **2011**, *40*, 239–241.
- (24) Ozawa, H.; Fujigaya, T.; Song, S.; Suh, H.; Nakashima, N. *Chem. Lett.* **2011**, *40*, 470–472.
- (25) Gao, J.; Loi, M. A.; Carvalho, E. J. F. D. C.; Santos, M. C. D. *ACS Nano* **2011**, *5*, 3993–3999.
- (26) Imin, P.; Imit, M.; Adronov, A. *Macromolecules* **2011**, *44*, 9138–9145.
- (27) Hopkins, J.; M. Dalrymple, S. A.; Parvez, M.; Keay, B. A. *Org. Lett.* **2005**, *7*, 3765–3768.
- (28) Canac, Y.; Chauvin, R. *Eur. J. Inorg. Chem.* **2010**, *2010*, 2325–2335.
- (29) Turlington, M.; Du, Y.; Ostrum, S. G.; Santosh, V.; Wren, K.; Lin, T.; Sabat, M.; Pu, L. *J. Am. Chem. Soc.* **2011**, *133*, 11780–11794.

(30) Dukovic, G.; Balaz, M.; Doak, P.; Berova, N. D.; Zheng, M.; Mclean, R. S.; Brus, L. E. *J. Am. Chem. Soc.* **2006**, *128*, 9004–9005.

(31) Izard, N.; Kazaoui, S.; Hata, K.; Okazaki, T.; Saito, T.; Iijima, S.; Minami, N. *Appl. Phys. Lett.* **2008**, *92*, 243112.

(32) Fariborz, M.; Nigel, G. J. R.; Wayne, C. G.; Rob, L.; Mark, L.; Craig, C.; George, C.; Thomas, H.; Still, W. C. *J. Comput. Chem.* **1990**, *11*, 440–467.

(33) Es, J. J. G. S. V.; Biemans, H. A. M.; Meijier, E. W. *Tetrahedron: Asymmetry* **1997**, *8*, 1825–1831.

(34) Lee, J.-Ik; Chu, H. Y.; Lee, H.; Oh, J.; Do, L.-Mi; Zyung, T.; Lee, J.; Shim, H.-Ku. *ETRI J.* **2005**, *27*, 181–187.

(35) Grisorio, R.; Mastrorilli, P.; Nobile, C. F.; Romanazzi, G.; Suranna, G. P.; Gigli, G.; Piliego, C.; Ciccarella, O. G.; Cosma, P.; Acierno, D.; Amendola, E. *Macromolecules* **2007**, *40*, 4865–4873.